JOURNAL OF THE ROYAL SOCIETY Interface

Impact of negatively charged patches on the surface of MHC class II antigen-presenting proteins on risk of chronic beryllium disease

James A Snyder, Eugene Demchuk, Erin C McCanlies, Christine R Schuler, Kathleen Kreiss, Michael E Andrew, Bonnie L Frye, James S Ensey, Marcia L Stanton and Ainsley Weston

J. R. Soc. Interface 2008 **5**, 749-758
doi: 10.1098/rsif.2007.1223

JOURNAL OF THE ROYAL SOCIETY Interface

J. R. Soc. Interface (2008) **5**, 749–758
doi:10.1098/rsif.2007.1223
Published online 23 October 2007

Impact of negatively charged patches on the surface of MHC class II antigen-presenting proteins on risk of chronic beryllium disease

James A. Snyder[1], Eugene Demchuk[2,*], Erin C. McCanlies[1], Christine R. Schuler[3], Kathleen Kreiss[3], Michael E. Andrew[1], Bonnie L. Frye[1], James S. Ensey[1], Marcia L. Stanton[3] and Ainsley Weston[1,3]

[1]*Health Effects Laboratory Division, and* [3]*Division of Respiratory Disease Studies, National Institute for Occupational Safety and Health, 1095 Willowdale Road, Morgantown, WV 26505, USA*

[2]*Division of Toxicology and Environmental Medicine, Agency for Toxic Substances and Disease Registry, 1600 Clifton Road, Atlanta, GA 30333, USA*

Chronic beryllium disease (CBD) is a granulomatous lung disease that occurs primarily in workers who are exposed to beryllium dust or fumes. Although exposure to beryllium is a necessary factor in the pathobiology of CBD, alleles that code for a glutamic acid residue at the 69th position of the *HLA-DPβ1* gene have previously been found to be associated with CBD. To date, 43 *HLA-DPβ1* alleles that code for glutamic acid 69 (E69) have been described. Whether all of these E69 coding alleles convey equal risk of CBD is unknown. The present study demonstrates that, on the one hand, E69 alleloforms of major histocompatibility complex class II antigen-presenting proteins with the greatest negative surface charge convey the highest risk of CBD, and on the other hand, irrespective of allele, they convey equal risk of beryllium sensitization (BeS). In addition, the data suggest that the same alleles that cause the greatest risk of CBD are also important for the progression from BeS to CBD. Alleles convey the highest risk code for E26 in a constant region and for E69, aspartic acid 55 (D55), E56, D84 and E85 in hypervariable regions of the HLA-DPβ1 chain. Together with the calculated high binding affinities for beryllium, these results suggest that an adverse immune response, leading to CBD, is triggered by chemically specific metal–protein interactions.

Keywords: HLA-DP; genetic epidemiology; beryllium sensitization; granulomas; free energy perturbation; molecular dynamics

1. INTRODUCTION

Beryllium is a strong lightweight metal with unique properties that make it ideal for myriad technological uses in pure metal form, as oxide ceramics and in various alloys (Kolanz 2001; Taylor *et al.* 2003). It has applications in, but is not limited to, the aerospace, automobile, biomedical, defence, electronics, fire prevention and telecommunications industries. Although exposure to beryllium is likely to be the highest among employees engaged in primary beryllium production, it is estimated that well over 100 000 US workers in diverse occupations are currently at risk of beryllium exposure (Henneberger *et al.* 2004; Newman *et al.* 2005*a*).

Exposure to beryllium can lead to immunologic sensitization (BeS) and cause a cell-mediated immunologic granulomatous lung disease (CBD). Sensitization is an immunologic response that is detected using a beryllium lymphocyte proliferation test (Stokes & Rossman 1991; Stange *et al.* 2004). Beryllium-sensitized individuals may be clinically evaluated for CBD with tests including bronchoalveolar lavage and transbronchial biopsy. Among two large series of epidemiologic studies, 10–100% of sensitized individuals were found to have CBD at the time when sensitization was identified, with others developing CBD later (Kreiss *et al.* 2007). It is not known whether all beryllium-sensitized individuals will eventually develop CBD (Newman *et al.* 2005*b*).

Workplace screening programmes for sensitization have enabled the identification of CBD in persons without apparent symptoms, often early in disease progression. Symptoms of CBD are generally nonspecific, including shortness of breath, cough and fatigue. Progression from BeS to CBD, and from subclinical disease to clinical impairment, is extremely variable. Many questions concerning exposure-associated

*Author for correspondence (edemchuk@cdc.gov).

Disclaimer. The findings and conclusions in this report are those of the authors and do not necessarily represent the views of the National Institute for Occupational Safety and Health or the Agency for Toxic Substances and Disease Registry.

Received 9 September 2007
Accepted 27 September 2007

risks, disease mechanisms and the natural history of BeS and CBD remain to be answered (Newman *et al.* 2005*b*; Kreiss *et al.* 2007). It is important to keep in mind that BeS and CBD result only from exposure to beryllium particles, irrespective of the exposed person's genotype (Fireman *et al.* 2003; Infante & Newman 2004). However, it has been found that beryllium-exposed workers who subsequently developed BeS or CBD were significantly more likely to carry an *HLA-DPβ1*E69* gene, that is an allele coding for a glutamic acid residue in the 69th position (E69) of the mature protein (Richeldi *et al.* 1993, 1997; Wang *et al.* 1999, 2001; Saltini *et al.* 2001; Rossman *et al.* 2002; Maier *et al.* 2003; McCanlies *et al.* 2004).

E69 belongs to one of six functionally important hypervariable regions (HVRs) on the HLA-DPβ1 chain of MHC class II antigen-presenting proteins. HVRs on HLA-DPβ1 have been implicated in a number of immunopathological disorders, including sarcoidosis, multiple sclerosis, rheumatoid arthritis, asthma, endometriosis, celiac disease, myasthenia gravis and others (Hoffmann & Valencia 2004; Shiina *et al.* 2004). Early molecular genetics reports, although constrained by small populations and lack of X-ray data, alluded to the pivotal structural role of HVRs in CBD (Richeldi *et al.* 1993; Fontenot *et al.* 2000). Recently, a new structural model for HLA-DP has been proposed (Snyder *et al.* 2003). This model, developed with full atomistic details, has facilitated formulation of new epidemiologic hypotheses (Weston *et al.* 2005*a*) that were tested in the present study using blood samples from a large cohort of 854 beryllium-exposed workers.

2. MATERIAL AND METHODS

2.1. Research subjects

We tested these hypotheses in a population of current and former beryllium industry employees. The group comprised 84 individuals with CBD, 72 with BeS and 698 without BeS or CBD. Industry employees from three primary production facilities were recruited between August 1999 and December 2001. Informed consent documents, approved by the National Institute for Occupational Safety and Health's Human Studies Review Board, were administered and signed. All genetic data are protected by an Assurance of Confidentiality (308d) obtained by NIOSH from the Centers for Disease Control and Prevention.

2.2. Exon 2 of HLA-DPβ1 gene sequencing and PCR amplification

DNA samples were isolated (McCanlies *et al.* 2004) and analysed using allele-specific DNA sequencing that used four specific forward primers (5′AATTACGTGT ACCAGTTACG3′, 5′ATTACCTTTTCCAGGGAC G3′, 5′AATTACGTGTACCAGGGAC3′, 5′ATTAC GTGCACCAGTTACG3′) and three specific reverse primers (5′GGTCACGGCCTCGTC3′, 5′GTCATG GGCCCGCC3′, 5′GGTCATGGGCCCGAC3′). These sequences were derived from information contained in the GenBank entry with accession number X02228. A detailed description of *HLA-DPβ1* gene sequencing, using a Beckman–Coulter CEQ 8000 automated sequencer (Fullerton, CA), was previously reported (Weston *et al.* 2005*b*).

2.3. DNA sequence attribution and statistical analyses

The SEQLAB program (Accelrys, Inc., San Diego, CA) was used to compare DNA sequence read out with a library of *HLA-DPβ1* nucleotide sequences identical to those found on the IMGT/HLA Web site (Robinson *et al.* 2003). Mantel–Haenszel analysis of odds ratios associated with CBD, BeS and potential progression from BeS to CBD and alleles coding different HLA-DP molecules that have E69 were determined by logistic regression (Clayton & Hills 1993).

2.4. Molecular dynamics and free energy perturbation

There are no experimentally determined coordinates for HLA-DP in the Protein Data Bank (http://www.rcsb.org/pdb). We modelled the extracellular part of HLA-DP by homology to a known HLA species (Snyder *et al.* 2003). All molecular dynamics (MD) simulations were performed using CHARMM v. 30 with the CHARMM22 force field (Brooks *et al.* 1983; MacKerell *et al.* 1998). Each HLA-DP model contained 367 residues. Titratable groups on the protein were assigned standard protonation states at pH 7.0, that is the aspartic acid and glutamic acid residues were charged negatively (−1), and the lysine and arginine residues positively (+1). Since acidic residues outnumber basic on the extracellular part of HLA-DP, the simulated protein fragment had a strongly acidic isoelectric point. The total negative charge on the protein was neutralized using counter ions, which were solvated in an octahedral box of water surrounding the protein. Periodic boundary conditions were applied. Water molecules were represented by the TIP3P model (Jorgensen *et al.* 1983). Each positively charged beryllium (II) ion (Be^{2+}) was positioned by locating a point on the solvent-accessible surface for which the negative electrostatic potential was of the greatest magnitude. A Na^+ ion was used to balance the remaining unit charge, if any, after all Be^{2+} ions were added. For example, the HLA-DPα1*01031/DPβ1*1701 complex was solvated with 34 661 water molecules, 13 Be^{2+} ions and one Na^+ ion. The dimension of the cuboid box before truncation was 131.644 Å. The system was first subjected to 5000 steps of the steepest descent minimization. Initial velocities were assigned based on the Gaussian distribution of the Cartesian components of velocities at 100 K, and the system was heated from 100 to 300 K for 15 ps in a constant volume (NVT) ensemble. This was followed by simulations in an extended constant pressure (NPT) ensemble coupled to external thermostat and barostat. The leapfrog Verlet integrator, isotropic atmospheric Langevin piston pressure (Feller *et al.* 1995) with piston mass of 500 amu and Hoover thermal piston coupling (Hoover 1985) at 298 K were applied. The integration time step was 1 fs. The long-range

electrostatic interactions were modelled without truncation using the particle-mesh Ewald (PME) summation method (Darden *et al.* 1993; Essmann *et al.* 1995), with Gaussian width κ of 0.667 Å^{-1}, a fourth-order β-spline interpolation, and a fast Fourier transform grid with the number of grid points in the x-, y- and z-direction each set to 144. The dielectric constant was 1 for the electrostatic interactions. The real space non-bonded interaction cut-off was 10 Å. The SHAKE algorithm (Ryckaert *et al.* 1977) was applied to eliminate high-frequency degrees of freedom. To prevent protein structure from deformation under strong interactions with divalent ions, the C and C_α backbone atoms were restrained using a harmonic potential with force constant of 500 kcal mol^{-1} Å^{-2}, which was maintained for the entire duration of the simulation. Before production of free energy perturbation (FEP) simulations began, each protein system has been simulated under conditions identical to the FEP conditions for at least 1 ns (i.e. an extended-period equilibration was carried out), during which the convergence of residue fluctuations and potential energy of the system has been achieved.

FEP calculations were performed using the PERT module of CHARMM. The simulations were set up as described above, except the PME real space cut-off was increased to 14.0 Å. According to the theory of statistical mechanics, the free energy is calculated by slow transformation of the ion along a pathway of non-physical transitional states connecting the initial state of the system when the ion is physically present (1) and with the final state when the ion is completely phased out (0). The pathway is given by an artificial coupling parameter λ that is added to the force field. The coupling parameter controls interactions of the ion with all other atoms in the system, including water and protein. The interactions are complete in the initial state when the ion is present, and they vanish in the final state when the ion 'disappears'. The coupling parameter λ is incremented in small 'windows' of $\Delta\lambda = \lambda_{i+1} - \lambda_i$ along the pathway, e.g. on the interval from 1 to 0, so that the free-energy difference between final and initial states takes the form

$$A_{1\to 0} = -k_{\mathrm{B}}T\sum_{i=1}^{N}\ln\left\langle \exp\left(\frac{U_{\lambda_{i+1}} - U_{\lambda_i}}{k_{\mathrm{B}}T}\right)\right\rangle_{\lambda_i},$$

where U_{λ_i} is the potential energy of the system held in the state λ_i; $\langle\ldots\rangle_{\lambda_i}$ denotes averaging over an ensemble of configurations representing the state λ_i; and k_{B} and T are Boltzmann's constant and absolute temperature, respectively. In the present study, both the charge and the radius of the Be^{2+} ion were allowed to vanish. The perturbations were carried out in forward and reverse directions. The interval of dynamic coupling parameter λ was divided equally into 50 parts, with each window of 0.02, respectively. Each λ_{i+1} trajectory was started from the last configuration of the previous window. For each window, 1 ps of pre-equilibration was performed, followed by 1 ps of data collection. The final energy values were taken as the accumulated sum of the forward and backward energies from each window. The FEP calculations for each HLA complex consisted of a total of 100 ps. The total CPU time required for the FEP calculations, including the initial system equilibration, exceeded 240 days on a Verari Linux Cluster, using two nodes, each node having two Intel Xeon 3.06 GHz processors.

2.5. Beryllium ion parametrization

In molecular mechanics, interatomic non-bonded interactions are usually described by the Lennard-Jones 12–6 potential derived by adjusting the internuclear separation σ (Å) of the pair of atoms at zero potential energy and the potential well depth ε (kcal mol^{-1}) at that minimum, such that macroscopic (time-averaged) properties of the system are reasonably reproduced. The key properties of metal cations include free energy of solvation and radial distribution functions. Both properties are reasonably well reproduced by the CHARMM22 force field for major physiological metals. These include divalent cations of common alkaline earth metals, such as magnesium and calcium. A smaller-sized beryllium, however, has not been appropriately parametrized. Its small size, in fact, prevents perfect parametrization within the CHARMM force field philosophy (Periole *et al.* 1997). The small size sets off a high charge density (ionic potential) on beryllium (II), which attributes unusual covalent properties to beryllium compounds compared to the heavier elements in the second group. For instance, beryllium chloride is covalent, while magnesium chloride and calcium chloride are ionic. As a result, the physicochemical properties of beryllium are better captured by *ab initio* quantum mechanics rather than molecular mechanics (Marx *et al.* 1997; Pavlov *et al.* 1998; Martínez *et al.* 1999; Asthagiri & Pratt 2003). At present, the use of quantum mechanics in FEP calculations is computationally prohibitive. We relied on a less accurate but computationally affordable molecular mechanical approach as implemented in CHARMM. New parameters for Be^{2+} were developed following the standard CHARMM recipe (MacKerell *et al.* 1998). Using the MD and FEP techniques described above, a range of σ and ε pairs applicable to Be^{2+} was scanned in a series of 200 ps test runs in an NVT ensemble containing 998 water molecules and one Be^{2+} ion. For developing new parameters, we first required the geometrical properties of simulated systems to unconditionally match available structural information on beryllium hydration as given by radial distribution functions of Be^{2+} (Marx *et al.* 1997). Having the geometrical properties correct, a set of parameters with a closest match to the experimental solvation energy of Be^{2+} (Gomer & Tryson 1977; Marcus 1994) was found. It appeared that stereochemical and thermochemical properties of solvated Be^{2+} cannot be perfectly matched together using the same σ and ε of the classical Hamiltonian. Augmented with new Be^{2+} parameters ($\sigma = 1.60362$ Å and $\varepsilon = 0.0090$ kcal mol^{-1}), the classical force field approach of CHARMM underestimated the absolute solvation free energy of Be^{2+} by 16–17% compared with the experimental free energy of beryllium hydration, which has been estimated as -563 kcal mol^{-1}

(Gomer & Tryson 1977) and −572 kcal mol^{-1} (Marcus 1994). Nevertheless, the obtained level of accuracy is by 1–11% better than previously reported (Periole *et al.* 1997). Moreover, the obtained free-energy errors were systematic. Systematic errors on absolute energies are known to cancel out, if thermodynamic calculations of the initial and final states are carried out under similar conditions, and then a *relative* free energy is calculated as a difference between the two states. At the same time, the developed parameters excellently reproduced Be–O radial distribution functions of Be^{2+} in water (Marx *et al.* 1997). Using the developed parameters, a simulated first solvation shell Be–O distance of 1.665 Å was in best agreement with experimental 1.67 Å (Yamaguchi *et al.* 1986) and with *ab initio* calculated 1.66±0.06 Å (Marx *et al.* 1997), 1.65 Å (Pavlov *et al.* 1998; Martínez *et al.* 1999) and 1.64±0.06 Å (Asthagiri & Pratt 2003). Since the right hydration structure of the inner solvation shell is a critical property of the ion, and the analysis of Be^{2+} affinity on HLA involves relative, not absolute free energies, the developed Lennard-Jones parameters represent a fair approximation in aqueous simulations of Be^{2+}. In the future, representation of Be^{2+} within the CHARMM framework may become even more accurate, as new polarizable force fields that accurately describe charge transfer and polarization are developed (Patel & Brooks 2006; Geerke & van Gunsteren 2007; Lopes *et al.* 2007).

2.6. Electrostatic calculations

The electrostatic potential was calculated using the University of Houston Brownian Dynamics program (Davis *et al.* 1991; Madura *et al.* 1995). The Insight II program (Accelrys, Inc., San Diego, CA) was used to generate the potential difference surface maps. The electrostatic potential was calculated by numerically solving the linearized Poisson–Boltzmann equation using a finite-difference method. The low-dielectric macromolecule (protein interior) was imbedded in a high-dielectric continuum environment (water exterior). A solution with charged ions was simulated having an assigned ionic strength of 0.145, which typifies conditions at the physiological pH. Using an ionic radius of 2.0 Å for the solvated ions, an ion exclusion layer was constructed around the solvent-accessible surface, having a null ionic strength inside, which determines the maximum distance which a typical ion can approach the solvent-accessible surface. The assigned temperature was 300 K. The resulting system was discretized on a grid, and the potential at the grid points was solved iteratively starting from the Debye–Hückel boundary conditions. To improve the accuracy of calculated potentials, a method of grid focusing was used. This involved three additional calculations in which the molecule was allowed to occupy a successively larger fraction of the cubic grid volume, so that values of the potential at the grid boundary could be calculated using the larger grid from each preceding calculation. The grid dimensions were selected to be 675 Å (spacing 2.7 Å per grid point), 385 Å (spacing 1.54 Å per grid point), 220 Å (spacing 0.88 Å) and 100 Å (spacing 0.50 Å per grid point). The interior and exterior dielectric constants were 2 and 78, respectively. The solute boundary was defined by a solvent-accessible surface generated using a rolling probe sphere radius of 1.4 Å. Partial atomic charges and radii were taken from the PARSE (Sitkoff *et al.* 1994) parameter set, which were originally optimized for proteins by fitting the solvation free energies of amino acid analogues. After the electrostatic potential grid was constructed, a solvent-accessible surface was generated using a rolling probe sphere radius of 0.9 Å, and the potential on the surface was interpolated at points on the surface from the grid. Electrostatic potentials reported in table 1 represent values interpolated at points in the metal-binding sites where a Be^{2+} ion was centred.

3. RESULTS AND DISCUSSION

Currently, there are more than 120 known variants of *HLA-DPβ1* collected in the EMBL IMGT/HLA database, http://www.ebi.ac.uk/imgt/hla/allele.html (Marsh 2007); 43 of these code for E69. A recent study demonstrates that individuals with BeS or CBD are significantly more likely to be homozygous for E69 than heterozygous[1] (odds ratio (OR), 3.1; 95% confidence interval (CI), 1.5–6.1), and that individuals with CBD are significantly more likely to have inherited an *HLA-DPβ1*E69* allele than individuals with BeS (OR, 2.3; 95% CI, 1.1–4.8; McCanlies *et al.* 2004). Based on these data, analyses of literature reports (Saltini *et al.* 2001; Rossman *et al.* 2002; Maier *et al.* 2003; McCanlies *et al.* 2003) and information from molecular modelling (Fontenot *et al.* 2000), we framed three formal hypotheses, details of which are elaborated elsewhere (Snyder *et al.* 2003; Weston *et al.* 2005*a*). We considered the two most abundant classes of *HLA-DPβ1*E69* alleles (frequencies of 0.28 and 0.56 of *HLA-DPβ1*E69* alleles, respectively), defined by the total negative charges of −9 or −7 on the titratable groups from the HVRs on the HLA molecules for which the alleles code (Rossman *et al.* 2002; Robinson *et al.* 2003; McCanlies *et al.* 2004; Weston *et al.* 2005*a*; Marsh 2007). The three hypotheses were: (i) alleles that code for HLA-DPβ1*E69 molecules and that have the greatest negative charge −9 convey higher risk of CBD than the more common HLA-DPβ1*E69 coding alleles that have a charge of −7, (ii) alleles that code for HLA-DPβ1*E69 molecules that have a charge of −9 convey equal risk of BeS to those that code for HLA-DPβ1*E69 molecules that have a charge of −7, (iii) alleles that code for HLA-DPβ1*E69 molecules that have a charge of −9 are more likely to predispose beryllium-sensitized subjects to progress to CBD than those that code for HLA-DPβ1*E69 molecules that have a charge of −7.

The data shown in figure 1*a* are the Mantel–Haenszel odds ratios for CBD and BeS of simple allele frequencies when alleles coding for HLA-DPβ1*E69 were classified by surface negative charge (−9 or −7). These data indicate that alleles that code for HLA-DPβ1*E69

[1]Homozygous implies having two copies of E69 (one on each chromosome), heterozygous implies having one copy of E69.

Table 1. Electrostatic potential (Φ), first-shell coordination and binding free energies relative to water ($\Delta\Delta G$), for the Be^{2+} ion positioned at β26/69, β55/56 and β84/85 sites.

HLA-DPβ1[a]			Φ (kT/e)	Be^{2+} coordination[b]	$-\Delta\Delta G^{c,d}$ (kcal mol^{-1})
	β26/β69				
*1701	E	E	−26.8	$(COO^-)_{\beta26,m}(COO^-)_{\beta69,m}(H_2O)_2$	51.2 (5.9)
*1701+P[e]	E	E	n.a.[f]	$(COO^-)_{\beta26,bi}(COO^-)_{\beta69,bi}(H_2O)$	90.0 (5.6)
*1301	E	E	−25.8	$(COO^-)_{\beta26,m}(COO^-)_{\beta69,m}(H_2O)_2$	51.1 (5.7)
*0201	E	E	−26.8	$(COO^-)_{\beta26,m}(COO^-)_{\beta69,m}(H_2O)_2$	47.7 (5.3)
*0401	E	K	−7.4	$(COO^-)_{\beta26,m}(H_2O)_3$	6.0 (6.5)
*0301	E	K	−4.7	$(COO^-)_{\beta26,m}(H_2O)_3$	4.8 (5.1)
	β84/β85				
*1701	D	E	−18.9	$(COO^-)_{\beta84,m}(COO^-)_{\beta85,bi}(H_2O)$	59.8 (6.6)
*1701+P	D	E	n.a.	$(COO^-)_{\beta84,m}(COO^-)_{\beta85,m}(H_2O)_2$	55.0 (5.1)
*1301	D	E	−18.9	$(COO^-)_{\beta84,m}(COO^-)_{\beta85,bi}(H_2O)$	66.6 (4.9)
*0201	G	G	n.a.	n.a.	n.a.
*0401	G	G	n.a.	n.a.	n.a.
*0301	D	E	−18.1	$(COO^-)_{\beta84,m}(COO^-)_{\beta85,bi}(H_2O)$	48.6 (7.1)
	β55/β56				
*1701	D	E	−12.3	$(COO^-)_{\beta55,m}(COO^-)_{\beta56,bi}(H_2O)$	50.0 (5.8)
*1701+P	D	E	n.a.	$(COO^-)_{\beta55,m}(OH)_{Y15pep}(H_2O)_2$	−3.0 (4.9)
*1301	A	A	n.a.	n.a.	n.a.
*0201	D	E	−11.3	$(COO^-)_{\beta55,m}(COO^-)_{\beta56,bi}(H_2O)$	53.6 (7.2)
*0401	A	A	n.a.	n.a.	n.a.
*0301	D	E	n.a.	n.a.	n.a.

[a] Alleles sorted by risk of CBD (*1701, with a charge of −9, is associated with the highest risk, and *0401, with a charge of −3, is associated with the least risk).
[b] Subscript m denotes monodentate and bi denotes bidentate with respect to coordination of COO^- with Be^{2+}.
[c] Values in parentheses are estimated errors calculated by taking the absolute difference between values from forward and backward FEP windowing.
[d] ΔG of hydration for Be^{2+} in water was calculated to be −472 kcal mol^{-1}.
[e] All calculations except '+P' were done with the antigen-binding pocket free of antigenic peptide.
[f] n.a., not applicable, or low.

molecules with a charge of either −9 or −7 are significantly associated with the risk of CBD, but that the risk associated with alleles coding for HLA-DPβ1*E69 molecules with a negative charge of −9 is more than twice that for −7 (OR, 2.8; 95% CI, 1.6–4.9). The data also indicate both −9- and −7-charged HLA-DPβ1*E69 are significantly associated with the risk of BeS, but that there is no difference between −7 and −9 alleles for risk of BeS (OR, 0.9; 95% CI, 0.4–2.1). The data also suggest that alleles coding for HLA-DPβ1*E69 with a charge of −9 are predictive of risk of CBD in individuals who are already sensitized (OR, 4.5; 95% CI, 1.6–12.5), but that alleles with a charge of −7 probably are not (OR, 2.2; 95% CI, 0.9–5.0); and that the difference between the two classes is significant (OR, 3.1; 95% CI, 1.2–7.9). Similarly, when the total charge associated with the diploid genotype was considered, genotypes, which code for the highest negative charge on the HLA-DPβ1 combinations, had the highest frequency among CBD cases (F=0.21; figure 1*b*). This difference was statistically significant compared with the control group (F=0.08, $p<0.0001$), as well as the BeS group (F=0.09, p=0.04).

To explain the observed statistically significant association between the charge on HLA and the risk of CBD and BeS, structural models of HLA-DP molecules for which the specific *HLA-DP* alleles code were developed (Snyder *et al.* 2003). These models revealed the surface charge patches as they relate to the HLA-DP antigen-binding pocket (McCanlies *et al.* 2003; Snyder *et al.* 2003). The difference between an HLA-DP molecule encoded by a low-risk allele (*HLA-DPβ1*0401*, charge −3) and a high-risk allele (*HLA-DPβ1*1701*, charge −9) was found to be dramatic, while differences between the high- and intermediate-risk alleles (e.g. *HLA-DPβ1*0201*, charge −7) were found to be less. A molecular electrostatic potential (MEP) difference plot depicts charge disparities (figure 2). Note that the disparities are large between the low-risk *HLA-DPβ1*0301*, which codes for negatively charged residues at positions β55, β56, β84, β85 and *HLA-DPβ1*1701* due to the absence of E69. However, a relatively modest difference is seen between *HLA-DPβ1*0201* and *HLA-DPβ1*1701*. These data suggest that negatively charged residues may provide an anchor in the bed of the protein for positively charged beryllium ions.

This hypothesis was tested using FEP techniques with all-atom models of HLA and explicit solvent. Several assumptions were made. Firstly, the study was carried out with titratable groups kept in their standard protonation states at pH 7.0. We did not consider complex pH-dependent polymeric beryllium structures that have been observed in pure water (Alderighi *et al.* 2000). Instead, we focused at chelating binding sites on HLA for mononuclear beryllium (II). Be^{2+} is well characterized in protein chelates (McCleskey *et al.* 2007). We tested the ability of Be^{2+} to bind on HLA. Secondly, to enhance sampling around the equilibrium

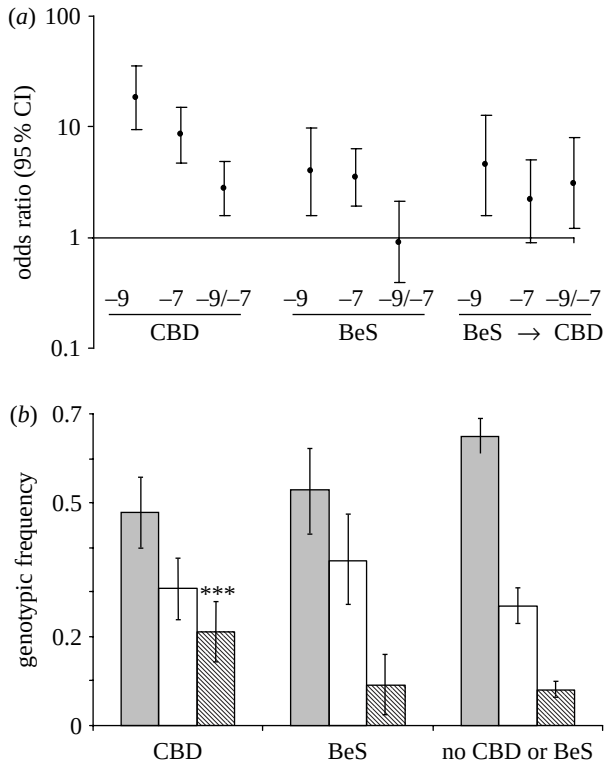

Figure 1. Comparisons of the HLA charge levels associated with allele frequencies and genotypes in groups of beryllium workers segregated by disease and beryllium sensitization. (*a*) Mantel–Haenszel analysis of odds ratios (ORs) associated with CBD, BeS and progression from BeS to CBD and *HLA-DPβ1* alleles coding for HLA-DP molecules that have E69. ORs indicated by −9 and −7 were calculated by comparing *HLA-DPβ1*E69* alleles with a surface charge in the antigen-binding pocket on the protein of either −9 or −7 with non-*HLA-DPβ1*E69* alleles as the referent category; ORs indicated by −9/−7 compare *HLA-DPβ1*E69* alleles encoding for a charge of −9 with *HLA-DPβ1*E69* alleles encoding for a charge of −7 as the referent category. Negative numbers refer to the charge on HLA molecules coded for by specific *HLA-DPβ1*E69* alleles. (*b*) An extension of the data shown in (*a*) was the development of a genotypic model to assess the impact of the combined charge for both alleles on the risk of BeS and CBD. A trend in the data clearly shows that the more the HLA molecules with high negative charge are encoded by the genotype, the higher the risk of disease in beryllium-exposed employees ($^{***}p<0.0001$ for CBD compared to the group with no CBD or BeS and $p=0.04$ for CBD compared to BeS). Genotype groupings are classified by total HLA negative charge for both alleles added together: filled bar, −10 to −12; open bar, −13 to −15; and striped bar, −16 to −18.

position, as given by X-ray coordinates, the C and C_α backbone atoms of HLA were restrained by a harmonic potential. On the one hand, it forced the system to extensively explore the phase space around equilibrium, to which the restraint-free side chain motions contribute most; and on the other hand, it prevented trapping of the system in transient local minima, which otherwise could be caused by multiple factors such as: slow motions along low-frequency modes of the protein; the unusually high, compared to other divalent ions, energetics of Be^{2+} solvation (Marcus 1994); imperfections in the molecular mechanical force field; and other artefacts of computational MD.

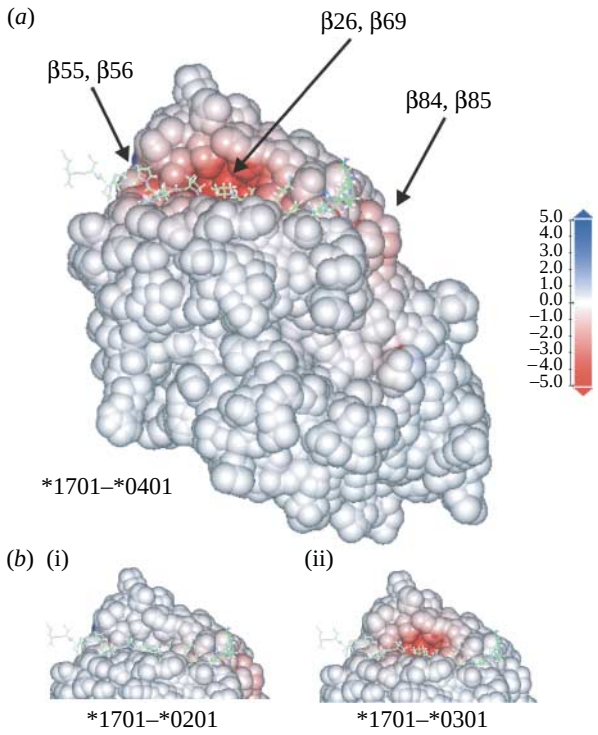

Figure 2. MEP difference surface maps. MEP was calculated for each HLA molecule. Since the molecules are encoded by alleles with mostly identical residues, the MEP maps are also similar, except for the regions of sequence variation. To focus at the differences, pairwise MEP map differences were calculated for each pair of molecules, which includes (*a*) a molecule coded for by *HLA-DPβ1*1701* allele minus the molecule coded for by *HLA-DPβ1*0401*, and similarly (*b*(i)) *1701–*0201 and (*b*(ii)) *1701–*0301. The scale indicates colour-coded intensities of the electrostatic potential (kT/e). The stick model is the immunodominant fragment of myelin basic protein. It depicts a typical position of antigenic peptide in the HLA-binding pocket.

The binding free energies for Be^{2+} were calculated by subtracting the free energies of solvation of the beryllium ion in water from free energies of the ions docked to the HLA-DP proteins for which the different alleles code (table 1). Three pairs of amino acid residues from HVRs (β26/69, β55/56, β84/85) that contribute most to the overall negative charge were considered. For HLA-DPβ1*1701, high-affinity chelation of Be^{2+} is seen at each amino acid pairing. The affinity mode for Be^{2+} at the β26/69 site of HLA-DPβ1*1701, in which $[Be(H_2O)_2]^{2+}$ is chelated by the two carboxyl groups of β-chain, is shown (figure 3). The chelate structure can be described as an almost ideal tetrahedron, which is in agreement with previously reported chelation modes for Be^{2+} in both natural (Plieger *et al.* 2004; McCleskey *et al.* 2007) and designer chelating agents (Plieger *et al.* 2005). For *HLA-DPβ1*E69* alleles that code for β-chains with reduced overall charge, the affinity for Be^{2+} binding is reduced at least on some of the sites (table 1).

For HLA-DPβ1*0401, which has not been associated with increased risk of BeS or CBD, Be^{2+}-binding affinity is low at each of the three sites. Interestingly, for the *HLA-DPβ1*0301*, which codes for K69 in the β-chain with a charge of −7, the Be^{2+}-binding affinity

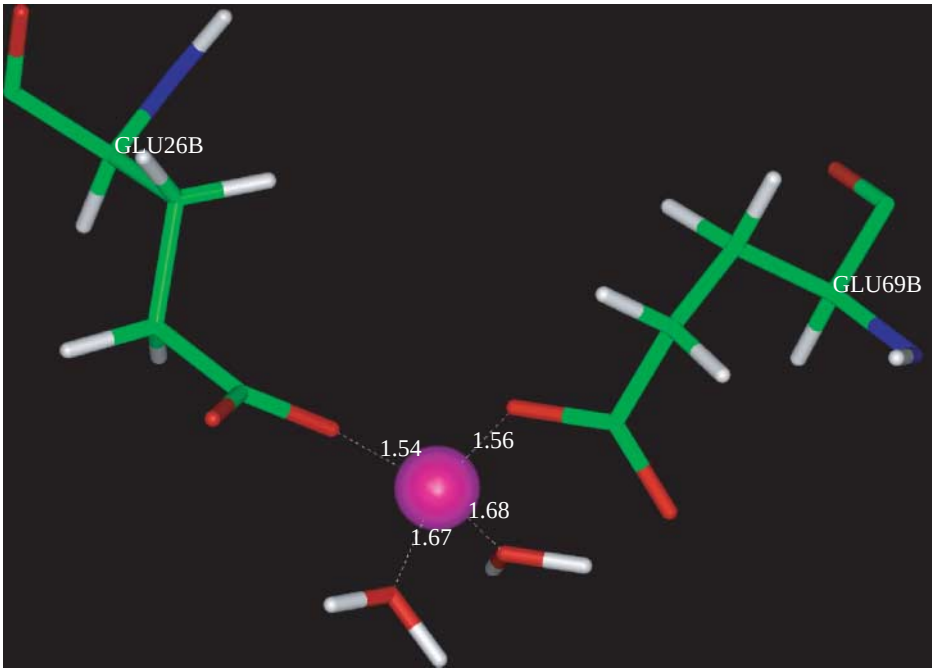

Figure 3. First shell of beryllium tetrahedron at the β26/69 site in the antigen-binding pocket of HLA-DPβ1*1701. Physicochemical properties of the chelate are expressed by the first line of table 1.

Table 2. First-shell coordination and binding free energies relative to water ($\Delta\Delta G$), for Mg^{2+}, Ca^{2+} and Zn^{2+} ions positioned at β26/69, β84/85 and β55/56 sites on HLA-DPβ1*1701.

binding site	coordination[a]	$-\Delta\Delta G^{b,c}$ (kcal mol^{-1})
	Mg^{2+}	
β69	$(COO^-)_{\beta26,bi}(COO^-)_{\beta69,bi}(H_2O)_2$	27.9 (5.8)
β84/85	$(COO^-)_{\beta84,m}(COO^-)_{\beta85,bi}(H_2O)_2$	40.4 (6.9)
β55/56	$(COO^-)_{\beta55,m}(COO^-)_{\beta56,bi}(H_2O)$	19.7 (6.4)
	Ca^{2+}	
β69	$(COO^-)_{\beta26,m}(COO^-)_{\beta69,bi}(H_2O)_3$	25.5 (7.4)
β84/85	$(COO^-)_{\beta84,m}(COO^-)_{\beta85,m}(H_2O)_2(O)_{\beta81}$	6.5 (4.2)
β55/56	$(COO^-)_{\beta55,m}(COO^-)_{\beta56,bi}(H_2O)_3$	33.7 (5.8)
	Zn^{2+}	
β69	$(COO^-)_{\beta26,bi}(COO^-)_{\beta69,bi}(H_2O)_3$	33.6 (4.9)
β84/85	$(COO^-)_{\beta84,bi}(COO^-)_{\beta85,bi}(H_2O)_2$	32.4 (8.2)
β55/56	$(COO^-)_{\beta55,m}(COO^-)_{\beta56,m}(H_2O)_3$	43.1 (4.5)

[a] Subscript m denotes monodentate and bi denotes bidentate with respect to coordination of COO^- with Be^{2+}.
[b] Values in parentheses are estimated errors calculated by taking the absolute difference between values from forward and backward FEP windowing.
[c] ΔG of hydration for Be^{2+} in water was calculated to be -472 kcal mol^{-1}.

at the D55/E56 doublet is unexpectedly low (ion dissociates). These data suggest that E69 significantly influences the conformation around the β55/56 doublet. Thus, these sites may be thermodynamically coupled.

Beryllium is an alkaline earth metal, along with magnesium (Mg) and calcium (Ca), with which it shares many similar physicochemical properties. Mg^{2+} and Ca^{2+} are biochemically important and amply present in the body. Then why does only Be^{2+} cause sensitization and disease? To understand the relevance of physiological divalent ions with respect to Be^{2+} binding on HLA-DP, relative binding energies for Mg^{2+}, Ca^{2+} and Zn^{2+} at the three aforementioned HVR binding sites were also calculated. It can be seen that Be^{2+} would effectively compete with more abundant physiologic divalent ions for binding at the HVR binding sites (table 2). Also, the bulkier divalent ions attract more water molecules in the binding cleft, making the chelate structures more susceptible to thermal fluctuations, and therefore making the anchor residues more accessible to peptide antigens. Superior binding energies of Be^{2+} suggest that it takes very small quantities of beryllium to displace these ions at their physiological concentration from the binding sites on HLA-DP. Therefore, even traces of beryllium may interact with the immune system of susceptible individuals.

The methods employed in the present study are insufficient to draw conclusions as to whether the beryllium ion alone acts as an antigen, or it changes the specificity of HLA to bind an endogenous peptide antigen. An additional possibility would be to consider the binding of beryllium to an antigenic peptide;

however, we are unaware of any HLA-DP-specific antigen or peptide at the time of this study. Also owing to small excluded volume, a short peptide is unlikely to bind Be^{2+} more strongly than the larger HLA. The impact of excluded volume on the energetics of ion binding is illustrated in table 1. Calculations denoted with '+P' were carried out with a peptide inserted in the antigen-binding pocket of HLA-DP. In the absence of known HLA-DP-specific peptides, an HLA-DR-specific peptide was used as a surrogate antigen. Presence of non-specific peptide improved the affinity of Be^{2+} binding at the major genetic marker, β69, by 76%. Binding affinity at the other two HVRs either did not change (β84/85) or was negligible (β55/56), which suggests that genetic markers at these sites contribute to CBD and BeS, perhaps either kinetically (by increasing local concentrations of beryllium ions around the major binding site β26/β69), or thermodynamically (owing to the aforementioned thermodynamic coupling to the major binding site). In either case, the conclusion holds as long as the surrogate peptide model holds, and since the sequence of a yet unknown HLA-DP-specific peptide is the most likely distinct from the surrogate, excluded solvent volume is the most likely reason for the observed changes in free energies of ion binding.

Our calculations do not suggest specificity of Be^{2+} binding to HLA-DPβ1*0401. Nevertheless, some exposed individuals bearing this allele have developed both BeS and CBD, albeit with frequencies much lower than genetically susceptible populations. Three possible explanations exist for the development of sensitization in the absence of genetic susceptibility associated with specific Be^{2+} binding: non-specific binding on HLA-DP and possibly other HLAs; binding to other proteins (Taylor-McCabe *et al.* 2006); or a yet unknown molecular mechanism. In other words, our results confirm a common epidemiological assertion that genetic susceptibility to BeS and CBD is a factor contributing to and exacerbating the medical condition rather than an exclusive reason for the disease. Note, besides Be^{2+}-binding sites in the antigen-binding pocket, there may be other metal-binding sites on HLA. Investigation of them is important, but outside the scope of the present study. The present study is focused on regions of variability in the *HLA-DP* genes, whose impact on BeS and CBD can be detected in epidemiologic studies. Metal-binding sites located outside the antigen-binding pocket would be constant among the alleles and therefore would equally contribute to susceptibility throughout the population. It is possible that a yet unknown constant site on HLA-DP causes the aforementioned background levels of BeS and CBD in *HLA-DPβ1*0401* alleles; however, such a site cannot be directly detected by genetic susceptibility studies. The same would be true for HLAs of other types as well and for any other protein in general. In fact, strong binding of beryllium (II) on non-immune-response proteins has been observed (McCleskey *et al.* 2007), but it has little to do with our current knowledge of CBD and BeS.

4. CONCLUSIONS

Epidemiologic studies have documented differing risks of specific HLA allelic groupings among beryllium-exposed workers for CBD, BeS and progression from BeS to CBD. These groupings can be distinguished by the surface charge and conformation of HLA using computational methods. The binding characteristics of specific HLA molecules suggest a physicochemical basis for the initiation of an immunologic reaction leading to CBD. In this scenario we present a hypothesis that the class II-associated invariant chain protein (CLIP), normally found in the antigen-binding groove and under normal circumstances competed off by an antigen, is displaced chemically by Be^{2+} in the case of HLA-DPβ1 molecules (Bangia & Watts 1995). Furthermore, it follows that CLIP is displaced more easily from HLA-DPβ*E69 that have a −9 charge than −7, and CLIP is displaced more readily by Be^{2+} from −7 HLA-DPβ1*E69 than HLA-DPβ1 with a lysine residue at the 69th position.

Altogether, the multidisciplinary approaches taken in the present study appear to provide insight into the molecular-genetic basis of variation in genetic susceptibility to beryllium health effects. These data have significant implications for genome-based risk assessment in occupationally related disease, especially as it relates to the exposure to metals (Bartell *et al.* 2000; Judd *et al.* 2003). It may be possible to use computational chemistry to identify other specific HLA molecules that have a unique ability to undergo adverse interaction with particular metals, e.g. cobalt, tungsten, titanium and others. Also, these data have potential implications for the development of interventions for metal-induced disease involving chelation and competitive inhibition of HLA-activated adverse immunologic reactions (Plieger *et al.* 2005, 2007). This general approach might also be applicable to other occupational and environmental diseases, like asthma, for which aetiology is obscure but associations with HLA genotypes have been observed (Newman-Taylor 2003; Shiina *et al.* 2004).

We thank the National Cancer Institute for use of computer time and technical support at the Advanced Biomedical Computing Center of the Frederick Cancer Research and Development Center. This study was wholly dependent on the help and participation of a large number of workers and former workers at several beryllium facilities. We greatly appreciate their participation. We thank the National Institute for Occupational Safety and Health's Human Studies Review Board for their guidance pertaining to molecular epidemiology in the workplace.

REFERENCES

Alderighi, L., Gans, P., Midollini, S. & Vacca, A. 2000 Aqueous solution chemistry of beryllium. In *Advances in inorganic chemistry*, vol. 50 (eds A. G. Sykes & A. H. Cowley), pp. 109–172. New York, NY: Academic Press.

Asthagiri, D. & Pratt, L. R. 2003 Quasi-chemical study of Be^{2+} (aq) speciation. *Chem. Phys. Lett.* **371**, 613–619. (doi:10.1016/S0009-2614(03)00227-6)

Bangia, N. & Watts, T. H. 1995 Evidence for invariant chain 85–101 (CLIP) binding in the antigen binding site of MHC class II molecules. *Int. Immunol.* **7**, 1585–1591. (doi:10.1093/intimm/7.10.1585)

Bartell, S. M., Ponce, R. A., Takaro, T. K., Zerbe, R. O., Omenn, G. S. & Faustman, E. M. 2000 Risk estimation and value-of-information analysis for three proposed genetic screening programs for chronic beryllium disease prevention. *Risk Anal.* **20**, 87–99. (doi:10.1111/0272-4332.00009)

Brooks, B. R., Bruccoleri, R. E., Olafson, B. D., States, D. J., Swaminathan, S. & Karplus, M. 1983 CHARMM: a program for macromolecular energy, minimization, and dynamics calculations. *J. Comput. Chem.* **4**, 187–217. (doi:10.1002/jcc.540040211)

Clayton, D. & Hills, M. 1993 *Statistical models in epidemiology*, pp. 175–185. New York, NY: Oxford University Press.

Darden, T., York, D. & Pedersen, L. 1993 Particle mesh Ewald: an N log (N) method for Ewald sums in large systems. *J. Chem. Phys.* **98**, 10 089–10 092. (doi:10.1063/1.464397)

Davis, M. E., Madura, J. D., Luty, B. A. & McCammon, J. A. 1991 Electrostatics and diffusion of molecules in solution: simulations with the University of Houston Brownian dynamics program. *Comput. Phys. Commun.* **62**, 187–197. (doi:10.1016/0010-4655(91)90094-2)

Essmann, U., Perera, L., Berkowitz, M. L., Darden, T., Lee, H. & Pedersen, L. G. 1995 A smooth particle mesh Ewald method. *J. Chem. Phys.* **103**, 8577–8593. (doi:10.1063/1.470117)

Feller, S. E., Zhang, Y. H., Pastor, R. W. & Brooks, B. R. 1995 Constant pressure molecular dynamics simulation: the Langevin piston method. *J. Chem. Phys.* **103**, 4613–4621. (doi:10.1063/1.470648)

Fireman, E., Haimsky, E., Noiderfer, M., Priel, I. & Lerman, Y. 2003 Misdiagnosis of sarcoidosis in patients with chronic beryllium disease. *Sarcoidosis Vasc. Diffuse Lung. Dis.* **20**, 144–148.

Fontenot, A. P., Torres, M., Marshall, W. H., Newman, L. S. & Kotzin, B. L. 2000 Beryllium presentation to CD4(+) T cells underlies disease-susceptibility HLA-DP alleles in chronic beryllium disease. *Proc. Natl Acad. Sci. USA* **97**, 12 717–12 722. (doi:10.1073/pnas.220430797)

Geerke, D. P. & van Gunsteren, W. F. 2007 Calculation of the free energy of polarization: quantifying the effect of explicitly treating electronic polarization on the transferability of force-field parameters. *J. Phys. Chem. B* **111**, 6425–6436. (doi:10.1021/jp0706477)

Gomer, R. & Tryson, G. J. 1977 An experimental determination of absolute half-cell emf's and single ion free energies of solvation. *Chem. Phys.* **66**, 4413–4424. (doi:10.1063/1.433746)

Henneberger, P. K., Goe, S. K., Miller, W. E., Doney, B. & Groce, D. W. 2004 Industries in the United States with airborne beryllium exposure and estimates of the number of current workers potentially exposed. *J. Occup. Environ. Hyg.* **1**, 648–659. (doi:10.1080/15459620490502233)

Hoffmann, R. & Valencia, A. 2004 A gene network for navigating the literature. *Nat. Genet.* **36**, 664. (doi:10.1038/ng0704-664)

Hoover, W. G. 1985 Canonical dynamics: equilibrium phase-space distributions. *Phys. Rev. A* **31**, 1695–1697. (doi:10.1103/PhysRevA.31.1695)

Infante, P. F. & Newman, L. S. 2004 Beryllium exposure and chronic beryllium disease. *Lancet* **363**, 415–416. (doi:10.1016/S0140-6736(04)15523-2)

Jorgensen, W. L., Chandrasekhar, J., Madura, J. D., Impey, R. W. & Klein, M. L. 1983 Comparison of simple potential functions for simulating liquid water. *J. Chem. Phys.* **79**, 926–935. (doi:10.1063/1.445869)

Judd, N. L., Griffith, W. C., Takaro, T. & Faustman, E. M. 2003 A model for optimization of biomarker testing frequency to minimize disease and cost: example of beryllium sensitization testing. *Risk Anal.* **23**, 1211–1209. (doi:10.1111/j.0272-4332.2003.00396.x)

Kolanz, M. E. 2001 Introduction to beryllium: uses, regulatory history, and disease. *Appl. Occup. Environ. Hyg.* **16**, 559–567. (doi:10.1080/10473220119088)

Kreiss, K., Schuler, C. R. & Day, G. A. 2007 Beryllium: a modern industrial hazard. *Annu. Rev. Publ. Health* **28**, 259–277. (doi:10.1146/annurev.publhealth.28.021406.144011)

Lopes, P. E. M., Lamoureux, G., Roux, B. & MacKerell, A. D. 2007 Polarizable empirical force field for aromatic compounds based on the classical drude oscillator. *J. Phys. Chem. B* **111**, 2873–2885. (doi:10.1021/jp0663614)

MacKerell Jr, A. D., Brooks, B., Brooks III, C. L., Nilsson, L., Roux, B., Won, Y. & Karplus, M. 1998 CHARMM: the energy function and its parameterization with an overview of the program. In *Encyclopedia of computational chemistry*, vol. 1 (eds P. V. R. Schleyer, N. L. Allinger, T. Clark, J. Gasteiger, P. A. Kollman, H. F. Schaefer & P. R. Schreiner), pp. 271–277. Chichester, UK: Wiley.

Madura, J. D. *et al.* 1995 Electrostatics and diffusion of molecules in solution: simulations with the University of Houston Brownian dynamics program. *Comput. Phys. Commun.* **91**, 57–95. (doi:10.1016/0010-4655(95)00043-F)

Maier, L. A. *et al.* 2003 Influence of MHC class II in susceptibility to beryllium sensitization and chronic beryllium disease. *J. Immunol.* **171**, 6910–6918.

Marcus, Y. 1994 A simple empirical model describing the thermodynamics of hydration of ions of widely varying charges, sizes, and shapes. *Biophys. Chem.* **51**, 111–127. (doi:10.1016/0301-4622(94)00051-4)

Marsh, S. G. E. 2007 Nomenclature for factors of the HLA system, update December 2006. *Tissue Antigens* **69**, 290–292. (doi:10.1111/j.1399-0039.2007.00807.x)

Martínez, J. M., Pappalardo, R. R. & Sánchez Marcos, E. 1999 First-pinciples ion–water interaction potentials for highly charged monatomic cations. Computer simulations of Al^{3+}, Mg^{2+}, and Be^{2+} in water. *J. Am. Chem. Soc.* **121**, 3175–3184. (doi:10.1021/ja9830748)

Marx, D., Sprik, M. & Parrinello, M. 1997 *Ab initio* molecular dynamics of ion solvation. The case of Be^{2+} in water. *Chem. Phys. Lett.* **273**, 360–366. (doi:10.1016/S0009-2614(97)00618-0)

McCanlies, E. C., Kreiss, K., Andrew, M. & Weston, A. 2003 HLA-DPβ1 and chronic beryllium disease: a HuGE review. *Am. J. Epidemiol.* **157**, 388–398. (doi:10.1093/aje/kwg001)

McCanlies, E. C., Ensey, J., Schuler, C., Kreiss, K. & Weston, A. 2004 The association between HLA-DPβ1^{Glu69}, chronic beryllium disease, and beryllium sensitization. *Am. J. Ind. Med.* **46**, 95–103. (doi:10.1002/ajim.20045)

McCleskey, T. M., Ehler, D. S., Keizer, T. S., Asthagiri, D. N., Pratt, L. R., Michalczyk, R. & Scott, B. L. 2007 Beryllium displacement of H^+ from strong hydrogen bonds. *Angew. Chem. Int. Ed.* **46**, 2669–2671. (doi:10.1002/anie.200604623)

Newman, L. S., Maier, L. A., Martyny, J. W., Mroz, M. M., VanDyke, M. & Sackett, H. M. 2005*a* Beryllium workers' health risks. *J. Occup. Environ. Hyg.* **2**, D48–D50. (doi:10.1080/15459620590957346)

Newman, L. S., Mroz, M. M., Balkissoon, R. & Maier, L. A. 2005*b* Beryllium sensitization progresses to chronic

beryllium disease: a longitudinal study of disease risk. *Am. J. Respir. Crit. Care Med.* **171**, 54–60. (doi:10.1164/rccm.200402-190OC)

Newman-Taylor, A. J. 2003 HLA phenotype and exposure in development of occupational asthma. *Ann. Allerg. Asthma Immunol.* **90**, S24–S27.

Patel, S. & Brooks, C. L. 2006 Fluctuating charge force fields: recent developments and applications from small molecules to macromolecular biological systems. *Mol. Simulat.* **32**, 231–249. (doi:10.1080/08927020600726708)

Pavlov, M., Siegbahn, P. E. M. & Sandstrom, M. 1998 Hydration of beryllium, magnesium, calcium, and zinc ions using density functional theory. *J. Phys. Chem. A* **102**, 219–228. (doi:10.1021/jp972072r)

Periole, X., Allouche, D., Daudey, J.-P. & Sanejouand, Y.-H. 1997 Simple two-body cation–water interaction potentials derived from *ab initio* calculations. Comparison to results obtained with an empirical approach. *J. Phys. Chem. B* **101**, 5018–5025. (doi:10.1021/jp9701855)

Plieger, P. G., John, K. D., Keizer, T. S., McCleskey, T. M., Burrell, A. K. & Martint, R. L. 2004 Predicting ^{9}Be nuclear magnetic resonance chemical shielding tensors utilizing density functional theory. *J. Am. Chem. Soc.* **126**, 14 651–14 658. (doi:10.1021/ja046712x)

Plieger, P. G. *et al.* 2005 Novel binding of beryllium to dicarboxyimidazole-based model compounds and polymers. *Inorg. Chem.* **44**, 5761–5769. (doi:10.1021/ic050680c)

Plieger, P. G., John, K. D. & Burrell, A. K. 2007 Encapsulating beryllium—synthesis, characterization and modeling of a chiral binaphthyldiimine–Be(II) complex. *Polyhedron* **26**, 472–474. (doi:10.1016/j.poly.2006.07.020)

Richeldi, L., Sorrentino, R. & Saltini, C. 1993 HLA-DPβ1 glutamate 69: a genetic marker of beryllium disease. *Science* **262**, 242–244. (doi:10.1126/science.8105536)

Richeldi, L., Kreiss, K., Mroz, M. M., Zhen, B. G., Tartoni, P. & Saltini, C. 1997 Interaction of genetic and exposure factors in the prevalence of berylliosis. *Am. J. Ind. Med.* **32**, 337–340. (doi:10.1002/(SICI)1097-0274(199710)32:4<337::AID-AJIM3>3.0.CO;2-R)

Robinson, J., Waller, M. J., Parham, P., de Groot, N., Bontrop, R., Kennedy, L. J., Stoehr, P. & Marsh, S. G. E. 2003 IMGT/HLA and IMGT/MHC: sequence databases for the study of the major histocompatibility complex. *Nucleic Acids Res.* **31**, 311–314. (doi:10.1093/nar/gkg070)

Rossman, M. D., Stubbs, J., Lee, C. W., Argyris, E., Magira, E. & Monos, D. 2002 Human leukocyte antigen class II amino acid epitopes. Susceptibility and progression markers for beryllium hypersensitivity. *Am. J. Respir. Crit. Care Med.* **165**, 788–794.

Ryckaert, J.-P., Ciccotti, G. & Berendsen, H. J. C. 1977 Numerical integration of the Cartesian equations of motion of a system with constraints: molecular dynamics of *n*-alkanes. *J. Comput. Phys.* **23**, 327–341. (doi:10.1016/0021-9991(77)90098-5)

Saltini, C. *et al.* 2001 Major histocompatibility locus genetic markers of beryllium sensitization and disease. *Eur. Respir. J.* **18**, 677–684. (doi:10.1183/09031936.01.00106201)

Shiina, T., Inoko, H. & Kulski, J. K. 2004 An update of the HLA genomic region, locus information and disease associations: 2004. *Tissue Antigens* **64**, 631–649. (doi:10.1111/j.1399-0039.2004.00327.x)

Sitkoff, D., Sharp, K. A. & Honig, B. 1994 Accurate calculation of hydration free energies using macroscopic solvent models. *J. Phys. Chem.* **98**, 1978–1988. (doi:10.1021/j100058a043)

Snyder, J. A., Tinkle, S. S., Weston, A. & Demchuk, E. 2003 Electrostatic potential on human leukocyte antigen: implications for putative mechanism of chronic beryllium disease. *Environ. Health Perspect.* **111**, 1827–1834.

Stange, A. W., Furman, F. J. & Hilmas, D. E. 2004 The beryllium lymphocyte proliferation test: relevant issues in beryllium health surveillance. *Am. J. Ind. Med.* **46**, 453–462. (doi:10.1002/ajim.20082)

Stokes, R. F. & Rossman, M. D. 1991 Blood cell proliferation response to beryllium: analysis by receiver-operating characteristics. *J. Occup. Med.* **33**, 23–28. (doi:10.1097/00043764-199101000-00009)

Taylor, T. P., Ding, M., Ehler, D. S., Foreman, T. M., Kaszuba, J. P. & Sauer, N. N. 2003 Beryllium in the environment: a review. *J. Environ. Sci. Health A* **38**, 439–469. (doi:10.1081/ESE-120016906)

Taylor-McCabe, K. J., Wang, Z. L., Sauer, N. N. & Marrone, B. L. 2006 Proteomic analysis of beryllium-induced genotoxicity in an Escherichia coli mutant model system. *Proteomics* **6**, 1663–1675. (doi:10.1002/pmic.200500190)

Wang, Z. L., Farris, G. M., Newman, L. S., Shou, Y. L., Maier, L. A., Smith, H. N. & Marrone, B. L. 2001 Beryllium sensitivity is linked to HLA-DP genotype. *Toxicology* **165**, 27–38. (doi:10.1016/S0300-483X(01)00410-3)

Wang, Z. L., White, P. S., Petrovic, M., Tatum, O. L., Newman, L. S., Maier, L. A. & Marrone, B. L. 1999 Differential susceptibilities to chronic beryllium disease contributed by different Glu69 HLA-DPβ1 and -DPα1 alleles. *J. Immunol.* **163**, 1647–1653.

Weston, A., Snyder, J., McCanlies, E. C., Schuler, C. R., Andrew, M. E., Kreiss, K. & Demchuk, E. 2005*a* Immunogenetic factors in chronic beryllium disease. *Mut. Res. Fund. Mol. Mech. Mutagen.* **592**, 68–78. (doi:10.1016/j.mrfmmm.2005.06.005)

Weston, A., Ensey, J. S. & Frye, B. L. 2005*b* DNA sequence determination of exon 2 of a novel *HLA-DPβ* allele, HLA-DPB1*0403. *DNA Seq.* **16**, 235–236.

Yamaguchi, T., Ohtaki, H., Spohr, E., Pálinkás, G., Heinzinger, K. & Probst, M. M. 1986 Molecular dynamics and X-ray diffraction study of aqueous beryllium(II) chloride solutions. *Z. Naturforsch. A* **41**, 1175–1185.